JOURNAL OF AIRCRAFT
Vol. 37, No. 6, November–December 2000

Aeroelastic Tailoring of Composite Wings Exhibiting Nonclassical Effects and Carrying External Stores

Frank H. Gern* and Liviu Librescu†
Virginia Polytechnic Institute and State University, Blacksburg, Virginia 24061-0219

Structural and aeroelastic tailoring applied to advanced straight and swept aircraft wings carrying external stores is addressed. The wing structure is modeled as a laminated composite plate exhibiting flexibility in transverse shear and warping restraint effects. The equations of motion and boundary conditions are obtained via Hamilton's variational principle and application of generalized function theory. For a comprehensive representation of the stores, their static weights and inertia terms are considered. Three-dimensional modified strip theory aerodynamics is employed, and the obtained eigenvalue/boundary value problems are solved using the extended Galerkin method. The model is used to investigate the implications of external stores and ply angle orientation on divergence, free vibration, and flutter. Within the context of aeroelastic tailoring, the influence of external stores attached to the wing structure has to be considered during the preliminary aircraft design phases.

Nomenclature

AR = wing aspect ratio, $2l/c$
a_0 = sectional lift-curve slope
b = wing semichord length, $c/2$
$C(k)$ = Theodorsen function, $F(k) + iG(k)$
c = wing chord length measured perpendicular to the reference axis
E_p = distance between center of gravity of store and wing elastic axis, positive aft
f = frequency of oscillation
f_2, g_2 = two-dimensional displacement measures [Eq. (3b)]
G_{12}, G_{13} = in-plane shear modulus, transverse shear modulus
g = gravity acceleration
h = plunging displacement, positive upward
K_p = pitching radius of gyration of the store about its center of gravity
k = reduced frequency, $\omega b/V_n = \omega b/(V\cos\Lambda)$
$\mathcal{L}$ = sectional lift, positive upward
l = wing semispan measured along the reference axis
$\mathcal{M}$ = sectional aerodynamic torque about wing elastic axis, positive nose up
$\bar{Q}_{ij}$ = modified components of the elasticity tensor
q_n = component of the dynamic pressure normal to the reference axis, $\rho V_n^2/2$
R = transverse shear flexibility parameter, E_1/G_{13}
U_i = components of the three-dimensional displacement vector [Eqs. (3)]
V, V_n = airstream velocity and its component normal to the reference axis
x_0 = elastic axis position measured from the reference axis, positive aft
x_1, x_2, x_3 = chordwise, spanwise, and transverse coordinate normal to the midplane of the wing, respectively
δ, δ_D = variational operator, Dirac operator
ε = E_p/c
η, η_w = nondimensional spanwise location of wing store, x_2/l
θ, θ_0 = elastic twist angle, prescribed rigid wing angle of attack, positive nose up
Λ = sweep angle of the reference axis, positive for swept back
λ, λ_F = speed parameter, $V/b\omega_h$; flutter speed parameter, $V_F/b\omega_h$
μ_T, μ_w = $m_{\text{tipstore}}/m_{\text{wing}}, m_{\text{wingstore}}/m_{\text{wing}}$
Ω, Ω_F = frequency parameter, ω/ω_h; flutter frequency parameter, ω_F/ω_h
ω = circular frequency of oscillation
ω_h = uncoupled circular eigenfrequency in plunging for ply angle φ equals 0 deg

Subscripts and Superscript

S, W, T = stores, wing, tipstore
$,2$ = $\mathrm{d}(\,)/\mathrm{d}x_2$
$'$ = $\mathrm{d}(\,)/\mathrm{d}\eta$

Received 11 December 1998; revision received 4 April 2000; accepted for publication 12 May 2000.

*Deutsche Forschungsgemeinschaft Research Fellow, Department of Engineering Science and Mechanics; currently Research Assistant Professor, Center for Intelligent Material Systems and Structures. Member AIAA.
†Professor, Department of Engineering Science and Mechanics.

Introduction

BECAUSE modern civil and military aircraft wings are very often designed to carry external stores, external stores have gained special importance in the consideration of wing aeroelasticity. In the case of transport aircraft, these are mostly underwing carried stores, such as large and heavy engines and fuel tanks, or tip stores, such as winglets. Experimental investigation of the winglet influence on aeroelastic behavior revealed that most of the detrimental effects are due to the pure winglet mass and are not due to aerodynamic interactions.[1] Store attachments to fighter aircraft incorporate a wide variety of missile configurations, thus leading to literally hundreds of different store combinations. Very often, the stores exhibit dramatic changes in mass and inertia properties during one single mission due to the launch of missiles.[2]

The tremendous variety of possible store configurations dramatically influences static and dynamic aeroelastic behavior of aircraft wings, and the study of this problem has received prominence with the variable sweep fighter aircraft.[3,4] Because it is known that pylon-mounted stores strongly influence dynamic wing characteristics, the store pitching modes are of special importance from an aeroelastic point of view.[5] With store pitching modes being in the proximity of the wing's fundamental bending frequency, a critical aeroelastic coupling of the modes may occur, commonly referred to as wing-with-stores flutter.

As a result, for a successful design of the next generations of aerospace vehicles, and to eliminate the danger of the occurrence of any aeroelastic instability jeopardizing their imposed missions, it is imperative to have a perfect knowledge of the circumstances yielding the most critical aeroelastic instability. Toward this end, as a necessary requirement, modeling of the flight vehicle should

include the effect of distributed wing and tip stores on a composite wing.

The possibilities of beneficially tailoring the aeroelastic properties of wing structures by the employment of composite materials have been pointed out by recognized aeroelasticians[6,7] and were demonstrated by the development of the Grumman X-29 forward-swept wing aircraft. As shown in Refs. 8 and 9, nonclassical and often detrimental effects like warping inhibition and transverse shear flexibility of constituent materials are important parameters that have to be included in the aeroelastic model.

Structural Modeling

To investigate the effects of wing-mounted stores on aeroelasticity of advanced aircraft wings, a comprehensive structural model has been developed. Based on the concept of a shear deformable plate–beam model, the wing structure is idealized as a laminated composite plate, each constituent layer featuring different ply angles, material, and thickness properties. The total number of the constituent layers is denoted by N. The reference plane of the composite structure is selected to coincide with the plane interface between the two contiguous layers r and $r+1$ ($1 \le r \le N$). Its points are referred to a Cartesian system of in-plane coordinates (x_1, x_2). The coordinate x_3 is normal to the plane (x_1, x_2), with its positive direction upward. The x_1 and x_2 coordinates are referred to as chordwise and spanwise coordinates, respectively, whereas the reference plane is defined by $x_3 = 0$ (Fig. 1).

The equations of motion as well as boundary conditions are obtained via Hamilton's variational principle and application of generalized function theory to consider the spanwise location and properties of the attached stores exactly. To achieve a realistic representation of the store influence on static and dynamic behavior of the system, static weight and inertia of the attached stores are modeled, yielding the energy functional of a composite wing carrying external stores:

$$J = \int_{t_0}^{t_1} (\mathcal{T}_W - \mathcal{V}_W + \mathcal{T}_S - \mathcal{V}_S + \mathcal{W}_{NC})\, \mathrm{d}t \tag{1}$$

In Eq. (1) $\mathcal{T}$ and $\mathcal{V}$ denote the kinetic and potential energy of wing W and external stores S, respectively. The work done by the nonconservative forces, $\mathcal{W}_{NC}$, is obtained from the aerodynamic forces. From the stationary condition $\delta J = 0$, consistent with Eq. (1) and adopting the Einstein summation convention, one obtains

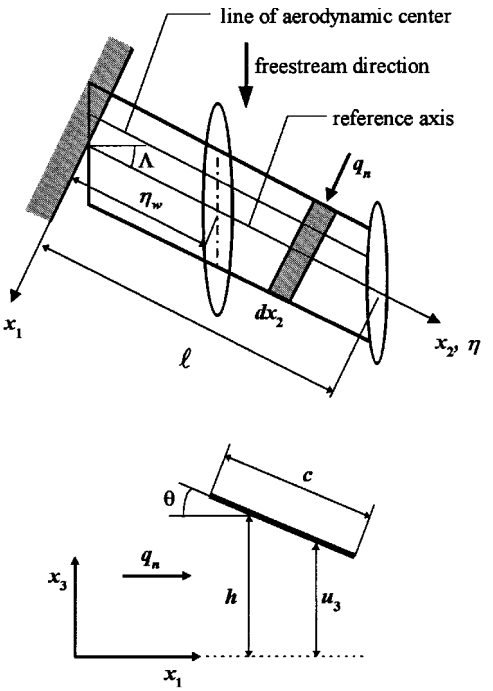

Fig. 1 Geometry of the swept-composite wing carrying external stores.

$$\delta J = 0 = \int_{t_0}^{t_1} \mathrm{d}t \underbrace{\left\{ \left(-\int_\tau \sigma_{ij}\delta U_{i,j}\,\mathrm{d}\tau + \int_\tau \rho(\mathcal{H}_i - \ddot{U}_i)\delta U_i\,\mathrm{d}\tau + \int_{\Omega_\sigma} \sigma_i \delta \tilde{U}_i\,\mathrm{d}\Omega \right)}_{\text{wing}} \right.$$

$$\left. + \underbrace{\sum_s \int_0^l \delta_D\left(x_2 - x_2^{(s)}\right)\left(-\int_{\tau_s} \rho^{(s)} \ddot{U}_i^{(s)} \delta U_i^{(s)}\,\mathrm{d}\tau + \mathcal{L}^{(s)}\delta h^{(s)} - \mathcal{M}^{(s)}\delta\theta^{(s)} + m^{(s)}\delta U_3^{(s)} \right)\mathrm{d}x_2}_{\text{external stores}} \right\} \tag{2}$$

In Eq. (2), the superposed dots denote time derivatives. The terms labeled with a tilde represent prescribed quantities, and the index s identifies the affiliation of the respective quantity to the external stores. $\mathcal{H}_i$ represents the component of the body force vector $\mathcal{H}$ (per unit mass), whereas σ_{ij} denotes the respective component of the stress tensor. The three-dimensional displacement components are given by

$$U_1 = x_3\theta(x_2; t) \tag{3a}$$

$$U_2 = u_2(x_2; t) + x_3[f_2(x_2; t) + x_1 g_2(x_2; t)] \tag{3b}$$

$$U_3 = h(x_2; t) - (x_1 - x_0)\theta(x_2; t) \tag{3c}$$

where, $\theta(x_2; t)$ is the elastic twist angle of a wing of rigid cross sections, whereas $h(x_2; t)$ is the vertical displacement (positive upward) of the respective cross section measured at the elastic axis and located at $x_1 = x_0[\equiv x_0(x_2)]$. See Refs. 10 and 11 for a detailed derivation of the three-dimensional displacement components.

For $f_2 = -h_{,2} - (x_0\theta)_{,2}$ and $g_2 = \theta_{,2}$, it results that $\gamma_{13} = \gamma_{23} = 0$. This is consistent with the traditional assumption of an infinite stiffness of the wing structure in transverse shear (Kirchhoff's theory).

In the case of a straight wing, the pitching angles $\theta^{(s)}$ of the stores coincide with the wing pitching angle θ. When considering swept wings of a sweep angle Λ, the reference coordinate system is being rotated with the wing by the sweep angle Λ (Fig. 1). However, in this case, note that the stores are always kept aligned parallel to the airflow. As a result, the three-dimensional displacement quantities of the stores have to be transformed to the rotated reference coordinate system to express the store inertia properties in a correct manner. This transformation yields

$$U_1^{(s)} = x_3\theta\cos\Lambda - u_2\sin\Lambda - x_3(f_2 + x_1 g_2)\sin\Lambda \tag{4a}$$

$$U_2^{(s)} = x_3\theta\sin\Lambda + u_2\cos\Lambda + x_3(f_2 + x_1 g_2)\cos\Lambda \tag{4b}$$

$$U_3^{(s)} = h - (x - x_0)[\theta\cos\Lambda - f_2\sin\Lambda - x_1 g_2\sin\Lambda] \tag{4c}$$

By employing the displacement components from Eqs. (3) and (4) and performing the indicated mathematical operations, the explicit form of Eq. (2) for the case of a composite aircraft wing carrying external stores is

$$\delta J = 0 = \int_{t_0}^{t_1} \mathrm{d}t \Bigg(\underbrace{\int_0^l [A_1\delta u_2 + A_2\delta f_2 + A_3\delta g_2 + (A_4 - \mathcal{M})\delta\theta + (A_5 + \mathcal{L})\delta h]\,\mathrm{d}x_2 + A_6}_{\text{energy functional of the clean composite wing}}$$

$$- \sum_s m^{(s)}\delta_D\left(x_2 - x_2^{(s)}\right)\left\{(\ddot{u}_2 + x_3\ddot{f}_2 + x_1x_3\ddot{g}_2)\delta u_2\right.$$

$$+ \left[x_3\ddot{u}_2 + \left(x_3^2 + K_p^{2(s)}\sin^2\Lambda\right)\ddot{f}_2 + \left(x_1x_3^2 + x_1K_p^{2(s)}\sin\Lambda\right)\ddot{g}_2 - K_p^{2(s)}\ddot{\theta}\sin\Lambda\cos\Lambda - E_p^{(s)}\ddot{h}\sin\Lambda\right]\delta f_2$$

$$+ x_1\left[x_3\ddot{u}_2 + \left(x_3^2 + K_p^{2(s)}\sin^2\Lambda\right)\ddot{f}_2 + \left(x_1x_3^2 + x_1K_p^{2(s)}\sin\Lambda\right)\ddot{g}_2 - K_p^{2(s)}\ddot{\theta}\sin\Lambda\cos\Lambda - E_p^{(s)}\ddot{h}\sin\Lambda\right]\delta g_2$$

$$+ \left[-K_p^{2(s)}\ddot{f}_2\sin\Lambda\cos\Lambda - x_1K_p^{2(s)}\ddot{g}_2\sin\Lambda\cos\Lambda + \left(x_3^2 + K_p^{2(s)}\cos^2\Lambda\right)\ddot{\theta}\right.$$

$$\underbrace{\left.\left. + E_p^{(s)}\ddot{h}\cos^2\Lambda\right]\delta\theta + \left(-E_p^{(s)}\ddot{f}_2\sin\Lambda - x_1E_p^{(s)}\ddot{g}_2\sin\Lambda + E_p^{(s)}\ddot{\theta}\cos\Lambda + \ddot{h}\right)\delta h\right\}}_{\text{kinetic energy of external stores}}$$

$$\underbrace{+ \sum_s \delta_D\left(x_2 - x_2^{(s)}\right)\left[\mathcal{M}^{(s)}\sin\Lambda\delta f_2 + x_1\mathcal{M}^{(s)}\sin\Lambda\delta g_2 - \mathcal{M}^{(s)}\cos\Lambda\delta\theta + \mathcal{L}^{(s)}\delta h\right]}_{\text{virtual work of external stores aerodynamics}}$$

$$\underbrace{+ \sum_s m^{(s)}g\,\delta_D\left(x_2 - x_2^{(s)}\right)\left[E_p^{(s)}\sin\Lambda\delta f_2 + x_1E_p^{(s)}\sin\Lambda\delta g_2 - E_p^{(s)}\cos\Lambda\delta\theta + \delta h\right]\Bigg)}_{\text{potential energy of external stores}} \tag{5}$$

where, $E_p^{(s)}$ is the distance between the center of gravity of the store and the wing elastic axis and $K_p^{(s)}$ is the pitching radius of gyration of the store about its center of gravity. The coefficients A_1–A_6 are displayed in Refs. 10 and 11 and, therefore, are not recorded here.

For the sake of completeness, Eq. (5) also displays the virtual work done by the nonconservative aerodynamic forces acting on the external stores. However, as it has been pointed out by Turner,[12] cases where store aerodynamics significantly influence the aeroelastic characteristics of the configuration are very rare. Therefore, store aerodynamics will not be considered in the following developments.

By collecting the terms associated with the respective variations δu_2, δf_2, δg_2, $\delta\theta$, and δh, and having in view that these variations have to be arbitrary and independent, Eq. (5) yields the equations of motion as well as the boundary conditions. From the stationary condition $\delta J = 0$, which concerns each instant belonging to the interval $[t_0, t_1]$, the equations of motion result as

$$\delta u_2\colon A_1 + \sum_s \delta_D\left(x_2 - x_2^{(s)}\right)\left[-m^{(s)}\left(\ddot{u}_2 + x_3\ddot{f}_2 + x_1x_3\ddot{g}_2\right)\right] = 0 \tag{6a}$$

$$\delta f_2\colon A_2 + \sum_s \delta_D\left(x_2 - x_2^{(s)}\right)\left\{-m^{(s)}\left[x_3\ddot{u}_2 + \left(x_3^2 + K_p^{2(s)}\sin^2\Lambda\right)\ddot{f}_2 + \left(x_1x_3^2 + x_1K_p^{2(s)}\sin\Lambda\right)\ddot{g}_2 - K_p^{2(s)}\ddot{\theta}\sin\Lambda\cos\Lambda - E_p^{(s)}\ddot{h}\sin\Lambda\right]\right.$$
$$\left. + \mathcal{M}^{(s)}\sin\Lambda + m^{(s)}gE_p^{(s)}\sin\Lambda\right\} = 0 \tag{6b}$$

$$\delta g_2\colon A_3 + \sum_s \delta_D\left(x_2 - x_2^{(s)}\right)x_1\left\{-m^{(s)}\left[x_3\ddot{u}_2 + \left(x_3^2 + K_p^{2(s)}\sin^2\Lambda\right)\ddot{f}_2 + \left(x_1x_3^2 + x_1K_p^{2(s)}\sin\Lambda\right)\ddot{g}_2 - K_p^{2(s)}\ddot{\theta}\sin\Lambda\cos\Lambda - E_p^{(s)}\ddot{h}\sin\Lambda\right]\right.$$
$$\left. + \mathcal{M}^{(s)}\sin\Lambda + m^{(s)}gE_p^{(s)}\sin\Lambda\right\} = 0 \tag{6c}$$

$$\delta\theta\colon A_4 + \sum_s \delta_D\left(x_2 - x_2^{(s)}\right)\left\{-m^{(s)}\left[-K_p^{2(s)}\ddot{f}_2\sin\Lambda\cos\Lambda - x_1K_p^{2(s)}\ddot{g}_2\sin\Lambda\cos\Lambda + \left(x_3^2 + K_p^{2(s)}\cos^2\Lambda\right)\ddot{\theta}\right.\right.$$
$$\left.\left. + E_p^{(s)}\ddot{h}\cos^2\Lambda\right] - \mathcal{M}^{(s)}\cos\Lambda - m^{(s)}gE_p^{(s)}\cos\Lambda\right\} = 0 \tag{6d}$$

$$\delta h\colon A_5 + \sum_s \delta_D\left(x_2 - x_2^{(s)}\right)\left[-m^{(s)}\left(-E_p^{(s)}\ddot{f}_2\sin\Lambda - x_1E_p^{(s)}\ddot{g}_2\sin\Lambda + E_p^{(s)}\ddot{\theta}\cos\Lambda + \ddot{h}\right) + \mathcal{L}^{(s)} + m^{(s)}g\right] = 0 \tag{6e}$$

It should be stressed that these equations of motion, obtained from a plate–beam model, are similar to the ones obtained for thin-walled beam models.[13] Because only the stiffness quantities are affected by the physical realization of the structure, all structural configurations, including plate–beam models, thin-walled beams, as well as the implementation of different types of stiffeners in the wing, can be investigated using the same set of equations. This was conjectured by several authors.[14,15] The modified plate–beam models (so-called box-beam models) employed by these authors are an intrinsic feature of the present structural model.

In addition, the geometrical and statical boundary conditions at the wing root and tip are obtained. For a cantilevered wing, the boundary conditions at the root ($x_2 = 0$) are purely geometrical and expressed as

$$u_2 = \tilde{u}_2 \tag{7a}$$

$$f_2 = \tilde{f}_2 \tag{7b}$$

$$g_2 = \tilde{g}_2 \tag{7c}$$

$$\theta = \tilde{\theta} \tag{7d}$$

$$h = \tilde{h} \tag{7e}$$

In the case of a clean wing tip, that is, no tip store, the boundary conditions at the wing tip ($x_2 = l$) are purely statical:

$$\delta u_2\colon T_{22}^{(0,0)} = \tilde{T}_{22}^{(0,0)} \tag{8a}$$

$$\delta f_2\colon T_{22}^{(0,1)} = \tilde{T}_{22}^{(0,1)} \tag{8b}$$

$$\delta g_2\colon T_{22}^{(1,1)} = \tilde{T}_{22}^{1,1)} \tag{8c}$$

$$\delta\theta\colon T_{12}^{(0,1)} - T_{23}^{(1,0)} = \tilde{T}_{12}^{(0,1)} - \tilde{T}_{23}^{(1,0)} \tag{8d}$$

$$\delta h\colon T_{23}^{(0,0)} = \tilde{T}_{23}^{(0,0)} \tag{8e}$$

When considering a store located at the wing tip, the boundary conditions at $x_2 = l$ change to kinetic ones, thus taking into account the mass, inertia properties, and aerodynamics of the tip store:

$$\delta u_2\colon T_{22}^{(0,0)} = -m^{(T)}(\ddot{u}_2 + x_3\ddot{f}_2 + x_1x_3\ddot{g}_2) \tag{9a}$$

$$\delta f_2\colon T_{22}^{(0,1)} = -m^{(T)}\Big[x_3\ddot{u}_2 + \Big(x_3^2 + K_p^{2(T)}\sin^2\Lambda\Big)\ddot{f}_2 + \Big(x_1x_3^2 + x_1K_p^{2(T)}\sin\Lambda\Big)\ddot{g}_2 - K_p^{2(T)}\ddot{\theta}\sin\Lambda\cos\Lambda - E_p^{(T)}\ddot{h}\sin\Lambda\Big] + \mathcal{M}^{(T)}\sin\Lambda + m^{(T)}gE_p^{(T)}\sin\Lambda \tag{9b}$$

$$\delta g_2\colon T_{22}^{(1,1)} = x_1\Big\{-m^{(T)}\Big[x_3\ddot{u}_2 + \Big(x_3^2 + K_p^{2(T)}\sin^2\Lambda\Big)\ddot{f}_2 + \Big(x_1x_3^2 + x_1K_p^{2(T)}\sin\Lambda\Big)\ddot{g}_2 - K_p^{2(T)}\ddot{\theta}\sin\Lambda\cos\Lambda - E_p^{(T)}\ddot{h}\sin\Lambda\Big] + \mathcal{M}^{(T)}\sin\Lambda + m^{(T)}gE_p^{(T)}\sin\Lambda\Big\} \tag{9c}$$

$$\delta\theta\colon T_{12}^{(0,1)} - T_{23}^{(1,0)} + x_0T_{23}^{(0,0)} = -m^{(T)}\Big[-K_p^{2(T)}\ddot{f}_2\sin\Lambda\cos\Lambda - x_1K_p^{2(T)}\ddot{g}_2\sin\Lambda\cos\Lambda + \Big(x_3^2 + K_p^{2(T)}\cos^2\Lambda\Big)\ddot{\theta} + E_p^{(T)}\ddot{h}\cos^2\Lambda\Big] - \mathcal{M}^{(T)}\cos\Lambda - m^{(T)}gE_p^{(T)}\cos\Lambda \tag{9d}$$

$$\delta h\colon T_{23}^{(0,0)} = -m^{(T)}\Big(-E_p^{(T)}\ddot{f}_2\sin\Lambda - x_1E_p^{(T)}\ddot{g}_2\sin\Lambda + E_p^{(T)}\ddot{\theta}\cos\Lambda + \ddot{h}\Big) + \mathcal{L}^{(T)} + m^{(T)}g \tag{9e}$$

Equations (6–9) represent the equations governing the aeroelastic equilibrium of advanced composite aircraft wings laminated of anisotropic layers and exhibiting transverse shear flexibility and warping inhibition. In addition, they include arbitrarily distributed external stores in the wing's spanwise and chordwise directions, as well as the aerodynamics of the stores. These equations, expressed in terms of the unknown displacement quantities $u_2(x_2; t)$, $f_2(x_2; t)$, $g_2(x_2; t)$, $\theta(x_2; t)$, and $h(x_2; t)$, yield a 10-order governing system of ordinary differential equations.

On discarding the influence of the in-plane components of body forces $F_2^{(0,0)}$, as well as in-plane rotatory inertia terms, that is, terms $I^{(0,0)}\ddot{u}_2$, $I^{(0,1)}\ddot{f}_2$, and $I^{(1,1)}\ddot{g}_2$, the displacement quantity $u_2(x_2; t)$ can be expressed in terms of $f_2(x_2; t)$, $g_2(x_2; t)$, $\theta(x_2; t)$, and $h(x_2; t)$, and, thus, be eliminated from the system. By this way, the system can be equivalently reduced to an eighth-order differential equation system in terms of the unknowns $f_2(x_2; t)$, $g_2(x_2; t)$, $\theta(x_2; t)$, and $h(x_2; t)$.

Constitutive Equations

The constitutive equations relating the generalized stress couples $T_{ij}^{(m,n)}$ with the strain measures have been obtained in Ref. 10. To establish the study of the effects of external stores within the context of aeroelastic tailoring, the composite wing is chosen to be fabricated of a finite number N of homogeneous layers. It is further assumed that the material of each layer is linearly elastic and that the bonding between the layers is perfect. The three-dimensional constitutive equations for a generally orthotropic elastic material can be expressed as

$$\begin{bmatrix}\sigma_{11}\\ \sigma_{22}\\ \sigma_{33}\\ \sigma_{23}\\ \sigma_{13}\\ \sigma_{12}\end{bmatrix} = \begin{bmatrix}\bar{Q}_{11} & \bar{Q}_{12} & \bar{Q}_{13} & 0 & 0 & \bar{Q}_{16}\\ \bar{Q}_{12} & \bar{Q}_{22} & \bar{Q}_{23} & 0 & 0 & \bar{Q}_{26}\\ \bar{Q}_{13} & \bar{Q}_{23} & \bar{Q}_{33} & 0 & 0 & \bar{Q}_{36}\\ 0 & 0 & 0 & \bar{Q}_{44} & \bar{Q}_{45} & 0\\ 0 & 0 & 0 & \bar{Q}_{45} & \bar{Q}_{55} & 0\\ \bar{Q}_{16} & \bar{Q}_{26} & \bar{Q}_{36} & 0 & 0 & \bar{Q}_{66}\end{bmatrix}\begin{bmatrix}\varepsilon_{11}\\ \varepsilon_{22}\\ \varepsilon_{33}\\ \gamma_{23}\\ \gamma_{13}\\ \gamma_{12}\end{bmatrix} \tag{10}$$

where $\bar{Q}_{ij}$ are the transformed elastic coefficients associated with the kth layer in the global coordinate system of the wing structure, and $\gamma_{ij} = 2\varepsilon_{ij}$, where $i \neq j$ and ε_{ij} are the components of the strain tensor.

Numerical Solution of the Static Aeroelastic System

As stated, the extended Galerkin method has been applied for a numerical solution of the problem. The displacement field is represented as the sum of a finite number of mode shape functions as

$$[f_2(\eta), g_2(\eta), \theta(\eta), h(\eta)]^T = \sum_{j=1}^{n}[F_j, G_j, T_j, H_j]^T \cdot \eta^j \tag{11}$$

where η is the nondimensional spanwise coordinate ($\eta = x_2/l$), whereas the constant factors F_j, G_j, T_j, and H_j are the modal amplitudes.

To establish trends, strip theory aerodynamics have been employed. However, note that application of the extended Galerkin method allows a three-dimensional integration of the aerodynamic forces and moments along the wing span. Therefore, the sectional lift-curve slope and aerodynamic center remain arbitrary and may vary from section to section.

For the static case, the aerodynamic terms $\mathcal{L}$ and $\mathcal{M}$ representing the sectional lift and aerodynamic torsional moment[16] are expressed as

$$\mathcal{L}(\eta) = q_n c a_0 \theta_{\text{eff}} \tag{12a}$$

$$\mathcal{M}(\eta) = q_n c e a_0 \theta_{\text{eff}} \tag{12b}$$

where $q_n = \rho_0 V_n^2/2 = q\cos^2\Lambda$ is the dynamic pressure component normal to the leading edge and $a_0 \equiv 2\pi AR/(AR + 4\cos\Lambda)$ is the lift-curve slope coefficient corrected to include the effects of a finite wing span and the wing sweep angle Λ. In Eq. (12), θ_{eff} is the effective sectional angle of attack given by

$$\theta_{\text{eff}} = \theta_0 + \theta - \frac{1}{l}\frac{\partial h}{\partial \eta}\tan\Lambda \tag{13}$$

With θ_0 denoting the angle of attack of the rigid-wing structure, Eq. (13) including aerodynamic bending/twist coupling describes the well-known wash-in and wash-out effects of swept-forward and swept-back wing configurations, respectively. By replacing Eqs. (11–13) into Eq. (5), an inhomogeneous matrix equation describing the static aeroelastic response of the wing is obtained:

$$[\boldsymbol{A}] \cdot [\boldsymbol{s}] = [\boldsymbol{r}] \tag{14}$$

In the static case, the matrix $\boldsymbol{A}$ is composed of the (real) stiffness matrix of the wing but contains also the (real) aerodynamic influence quantities in terms of the dynamic pressure q_n, whereas $\boldsymbol{s}$ represents the solution vector with $\boldsymbol{s} = [F_1, \ldots, F_n, G_1, \ldots, G_n, T_1, \ldots, T_n, H_1, \ldots, H_n]^T$. The right-hand vector $\boldsymbol{r}$ incorporates the inhomogeneous part of the aerodynamic forces associated with the angle of attack of the rigid wing and the influence of the external stores.

To obtain the divergence pressure, the determinant of matrix $\boldsymbol{A}$ has to be calculated, yielding a characteristic polynomial in q_n. The smallest positive value of q_n fulfilling the condition $\det \boldsymbol{A} = 0$ represents the divergence pressure $(q_n)_{\text{div}}$. Because for the static case, there is no contribution of the external stores to the matrix $\boldsymbol{A}$, it becomes now evident that the influence of the stores on the divergence speed of the wing is immaterial. Experimental results obtained by Runyan and Watkins[17] reveal an identical behavior.

Numerical Solution of the Dynamic Aeroelastic System

For simulation of the dynamic aeroelastic system, the unknown functions are represented as

$$[f_2(\eta; t), g_2(\eta; t), \theta(\eta; t), h(\eta; t)]^T = \sum_{j=1}^{n}[F_j, G_j, T_j, H_j]^T \cdot \eta^j \cdot e^{i\omega t} \tag{15}$$

For the dynamic case, the aerodynamic terms $\mathcal{L}$ and $\mathcal{M}$ representing the sectional lift and aerodynamic torsional moment[16] associated with an incompressible flowfield are expressed as

$$\mathcal{L}(\eta, t) = -\pi\rho\omega^2 b^3 \left\{ \frac{h}{b} L_{hh} + \frac{1}{l}\frac{\partial h}{\partial \eta} L_{hh'} + \theta L_{h\theta} + b\frac{1}{l}\frac{\partial \theta}{\partial \eta} L_{h\theta'} \right\} \tag{16}$$

$$\mathcal{M}(\eta, t) = \pi\rho\omega^2 b^4 \left\{ \frac{h}{b} M_{\theta h} + \frac{1}{l}\frac{\partial h}{\partial \eta} M_{\theta h'} + \theta M_{\theta\theta} + b\frac{1}{l}\frac{\partial \theta}{\partial \eta} M_{\theta\theta'} \right\} \tag{17}$$

In Eqs. (16) and (17), L_{hh}, $L_{hh'}$, ..., $M_{\theta\theta'}$ represent the aerodynamic coefficients.[16]

For the Theodorsen function $C(k)$, the approximation[18] was used, namely,

$$C(k) = F(k) + iG(k)$$
$$= \frac{0.021573 + 0.210400k + 0.512607k^2 + 0.500502k^3}{0.021508 + 0.251239k + 1.035378k^2 + k^3}$$
$$- i\frac{0.001995 + 0.327214k + 0.122397k^2 + 0.000146k^3}{0.089318 + 0.934530k + 2.481481k^2 + k^3} \tag{18}$$

where k is

$$k = \omega b / V_n = \omega b / V\cos\Lambda \tag{19}$$

This representation finally leads to a complex eigenvalue problem expressed in matrix form as

$$[\boldsymbol{A}] - \omega^2[\boldsymbol{B}] = \boldsymbol{0} \tag{20}$$

where $\boldsymbol{A}$ is the (real) stiffness matrix of the wing and $\boldsymbol{B}$ is the (complex) matrix representing the inertia terms of wing and external stores as well as the complex aerodynamic parameters of the wing. The real part of the complex valued quantity ω represents the circular frequency of the oscillation, whereas its imaginary part constitutes the damping factor δ.

The implemented solution methodology is based on the inversion of the complex $\boldsymbol{B}$ and subsequent calculation of complex eigenvalues and eigenvectors of the obtained system matrix $\boldsymbol{AB}^{-1}$. The flutter speed is calculated in a fast converging iteration process rendering zero the imaginary (damping) part of the complex eigenvalues.

Validation

To verify the accuracy of the flutter analysis, a number of comparisons for several test cases were conducted. The first comparison was made with Goland's cantilevered wing of $AR = 6.67$ as given in Ref. 19 and the subsequently appended correction of the flutter results in Ref. 20. The results reveal that the predictions for flutter speed and flutter frequency provided by the present approach, namely, 493.6 km/h and 12.02 Hz, are in excellent agreement with Goland's exact results (494 km/h and 11.25 Hz).

As another test case, the example of a straight aircraft wing of $AR = 6.16$ with attached tip weights, as given in Ref. 20, was investigated. In the calculations, two different chordwise positions of the center of gravity of the tip store were considered, namely, $\varepsilon_T = E_p^{(T)}/c = 0.0$ (case I) and $\varepsilon_T = 0.1$ (case II). Note that the original flutter investigation by Goland and Luke also included the free-body motion of the rigid fuselage, which is not subject of the present calculations. Nevertheless, the prediction of flutter speed and frequency of the first torsional mode for cases I and II is very accurate.

In both cases, flutter occurs in the classical way as binary wing bending/torsion flutter due to frequency coalescence and vanishing aerodynamic damping of the first torsional mode at a flight speed of 1055 km/h. In Refs. 15 and 21, it was observed that the first bending branch interacts with the rigid-body mode and flutters at an even lower speed (994 km/h). Because the free-body motion of the fuselage was discarded in this investigation, there is no such interaction and, as a consequence, the first torsional mode yields the lowest flutter speed.

In the present calculations, the warping inhibition of the cantilevered wing structure is taken into account. For this reason, flutter of the second bending mode, which was observed by Housner and Stein[15] to be the most critical mode of instability (943 km/h), occurs only at very high air speeds.[21] The inclusion of the warping terms does not influence the stability behavior of the first bending and torsional modes.

Numerical Illustrations

To study the effects of external stores within the context of aeroelastic tailoring, the wing structure is considered to be manufactured of a graphite–epoxy composite material. In this context, the ply angle φ represents the counterclockwise angle of rotation of the laminate with respect to the x_1 axis of the wing. For a single-layer composite wing, the material properties are given in Table 1.

The effect of the ply angle φ on the divergence speed is shown in Fig. 2 for a swept-back, swept-forward, and straight wing. Figure 2 shows the normalized divergence speed $(q_n)_D/(q_n)_D^*$ vs the ply angle φ, where $(q_n)_D^* = (q_n)_D|_{\Lambda=\varphi=0}$. It can be seen that, with increasing forward sweep, the range of ply angles for which divergence is not critical is decreased. Figure 2 also highlights the effect of the transverse shear flexibility of the material.

Free vibration and flutter of the wing are examined for different combinations of wing and tip stores whose nondimensional properties are given in Table 1.

The free vibration behavior of wings carrying external stores and exhibiting nonclassical effects such as transverse shear flexibility and warping inhibition can be obtained as a byproduct of the dynamic analysis described in the preceding section. For this purpose, the airflow density is set equal to zero, rendering the inertia matrix $\boldsymbol{B}$ real and, therefore, stating a self-adjoint eigensystem with purely real eigenvalues. Figure 3 shows the influence of warping restraint on the free vibration characteristics of the wing.

Table 1 Structural and material properties of wing and external stores

Parameter	Value
E_1	$30 \cdot 10^6$ psi
E_2	$0.75 \cdot 10^6$ psi
G_{12}	$0.45 \cdot 10^6$ psi
G_{13}	$0.37 \cdot 10^6$ psi
$R = E_1/G_{13}$	81.081
ν_{12}	0.25
ρ	14.3×10^6 lb · s^2/in.^{4}
$\mu_W = m^{(\text{wingstore})}/m^{(\text{wing})}$	0.3
$\mu_T = m^{(\text{tipstore})}/m^{(\text{wing})}$	0.1
$\varepsilon_W = E_p^{(\text{wingstore})}/c$	−0.4
$\varepsilon_T = E_p^{(\text{tipstore})}/c$	−0.4
$\eta_W = x_2^{(\text{wingstore})}/l$	0.5

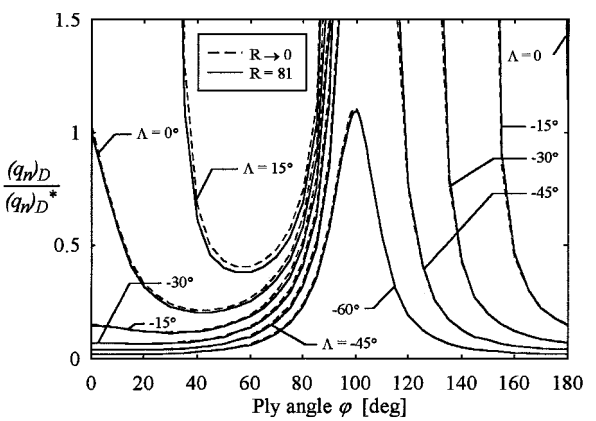

Fig. 2 Normalized divergence speed vs ply angle for swept and straight wings ($R = 81$, graphite epoxy and $R \to 0$, Kirchhoff's theory).

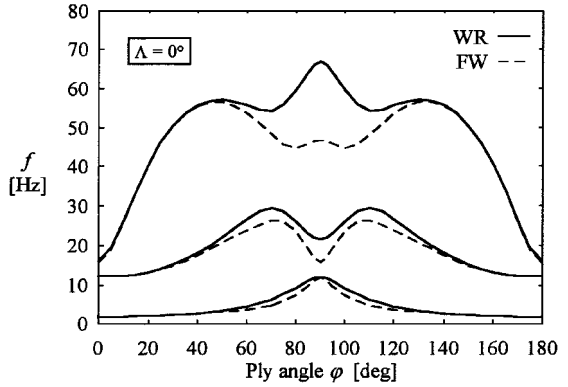

Fig. 3 Influence of warping restraint on the three lowest eigenfrequencies for a straight wing (FW = free warping and WR = warping restraint).

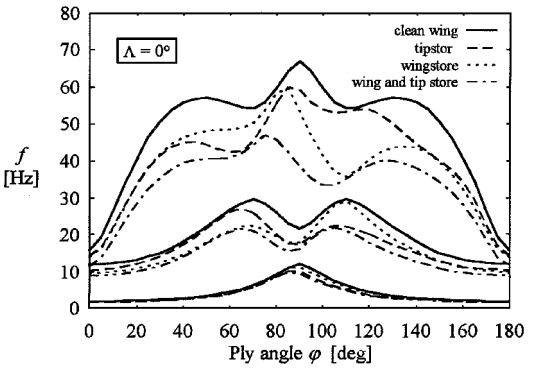

Fig. 4 Influence of external stores on the three lowest eigenfrequencies for a straight wing.

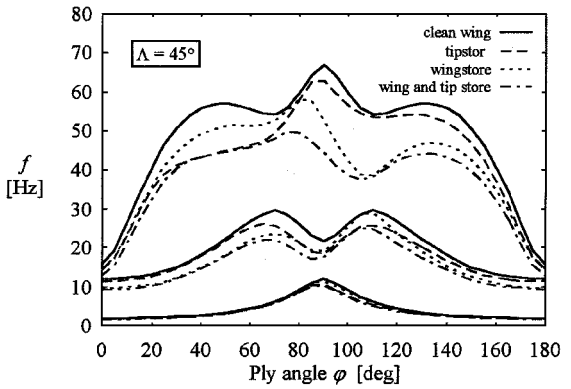

Fig. 5 Influence of external stores on the three lowest eigenfrequencies for a swept-back wing (Λ = 45 deg).

As shown in Fig. 4, vibration frequencies are lowered due to an increase of the generalized mass of the system by attaching external stores. However, because of the chordwise offset of the center of gravity of the stores, the symmetry of the vibration behavior with respect to the ply angle is destroyed. As can also be inferred from Fig. 4, the node lines of the higher-order vibrational modes are shifted with respect to changes in the ply angle orientation, as well as by increasing the generalized mass.[11] Figure 5 shows the free vibration behavior for a 45-deg swept-back wing of the same structural configuration. The trends shown in Figs. 4 and 5 are consistent with the ones experimentally and theoretically obtained by Lee and Lee.[22]

For a nonzero airflow density, matrix $\boldsymbol{B}$ becomes complex, rendering the eigenvalues of the system complex quantities. Figures 6 and 7 show flutter speed and flutter frequency, respectively, of a clean wing vs the ply angle φ for different sweep angles Λ. As it is shown,

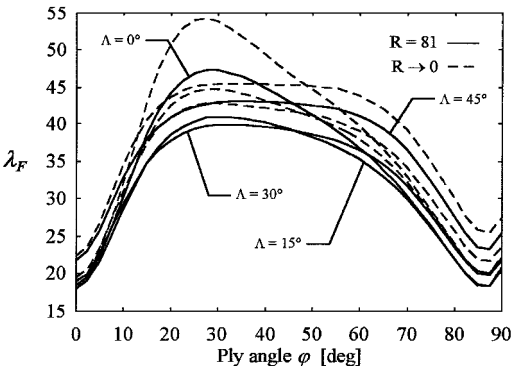

Fig. 6 Effect of ply angle φ and sweep angle Λ on flutter speed parameter $\lambda F = VF/b\omega h$ including transverse shear flexibility.

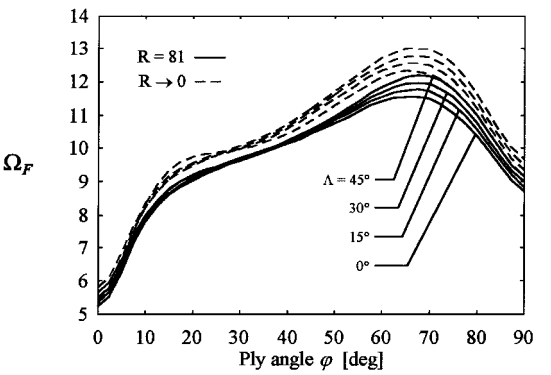

Fig. 7 Effect of ply angle φ and sweep angle Λ on flutter frequency parameter $\Omega F = \omega F/\omega h$ including transverse shear flexibility.

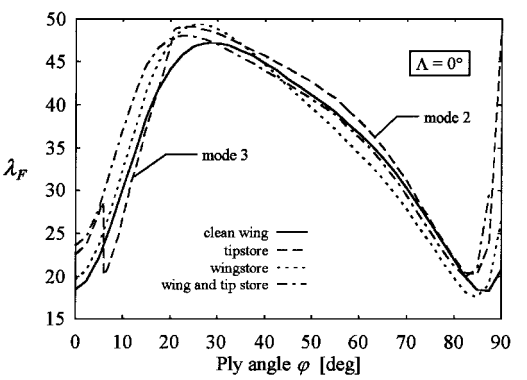

Fig. 8 Effect of ply angle φ on flutter speed parameter $\lambda F = VF/b\omega h$ for a straight wing (influence of external stores).

the maximum flutter speed of the wing is obtained for ply angles in the vicinity of 30 deg and is decreasing rapidly by approaching 0 deg as well as 90 deg. This trend is in perfect agreement with results obtained by Housner and Stein[15] using a finite difference method.

To highlight the effect of the transverse shear flexibility of the material on the flutter behavior of the wing, Figs. 6 and 7 also show the results obtained for the assumption of a transversely rigid material (Kirchhoff theory, $R \rightarrow 0$). As can be seen, neglecting the transverse shear flexibility leads to an overestimation of flutter speeds and flutter frequencies for all ply-angle orientations.

The influence of different combinations of wing and tip stores on flutter speed and frequency is shown in Figs. 8 and 9, respectively. Depending on the ply angle orientation, the presence of external stores may lead to a decrease or increase of the flutter speed with respect to the clean wing. Moreover, as can be seen from Figs. 8 and 9, changing the configuration of the external stores may even lead to a change in the critical flutter mode for certain ply angles. For the structural configuration shown in Figs. 8 and 9, the attachment of a

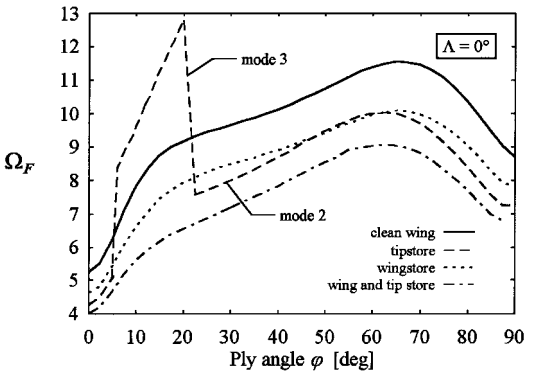

Fig. 9 Effect of ply angle φ on flutter frequency parameter $\Omega F = \omega F/\omega h$ for a straight wing (influence of external stores).

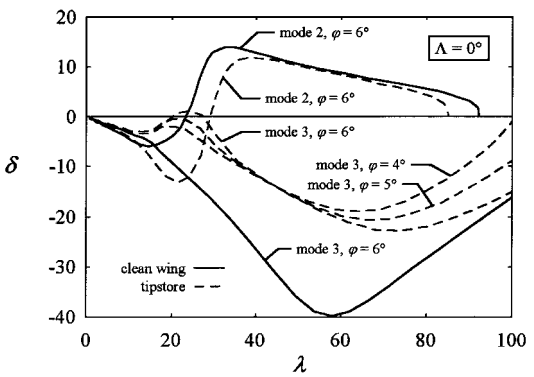

Fig. 10 Imaginary (damping) part δ of the complex eigenvalues of modes 2 and 3 vs flight speed parameter $\lambda = V/b\omega h$ at ply angle orientations near the discontinuity of the flutter boundary for a straight wing carrying a tip store.

tip store renders mode 3 to become the more critical flutter mode for ply angles between 6 and 20 deg, leading to a discontinuity of the flutter boundary in the vicinity of these ply angles. As a consequence, the flutter frequency jumps to the much higher frequency range of mode 3, whereas for all other ply angles and external stores combinations, mode 2 is the most critical flutter mode.

The discontinuity of the flutter boundary in the vicinity of a ply angle of $\varphi = 6$ deg can be explained by the existence of a hump mode (mode 3) for the wing carrying a tip store (Fig. 10). The critical flutter mode changes from mode 2 to mode 3 as φ is increased from 5 to 6 deg due a change in sign (from minus to plus) of the imaginary (damping) part δ of the complex eigenvalue of mode 3 for a flight speed parameter of $\lambda = 19.5$. A similar variation of the flutter speed vs the laminate ply angle was observed by Housner and Stein.[15] Notice that, for $\varphi = 6$ deg, mode 2 of the clean wing undergoes instability at a lower speed than mode 2 of the wing carrying a tip store. Nevertheless, for the wing with tip store, instability of mode 3 occurs at an even lower flight speed.

Note that this discontinuity of the flutter boundary occurs due to a change of the external stores configuration of the wing. As mentioned in the Introduction, such changes may occur during flight, for example, due to the launching of missiles or jettisoning of external tanks. Therefore, to it is very important to consider the possibility of different combinations of external stores attached to the wing also during ply-angle optimization for aeroelastic tailoring.

Figures 11 and 12 indicate that the observed discontinuity in the flutter speed does not occur for a 45-deg swept-back wing. The reason for this behavior is that, for the straight wing, the pitching mode of the tip store couples with mode 3 of the wing, thus producing the observed hump mode. To keep the stores aligned parallel to the airflow for the 45-deg swept-back wing, the store inertia properties are being transformed into the wing coordinate system [Eqs. (4a–4c)]. As a result, the interaction of the store pitch with mode 3 becomes weaker, causing the hump mode to disappear. Therefore,

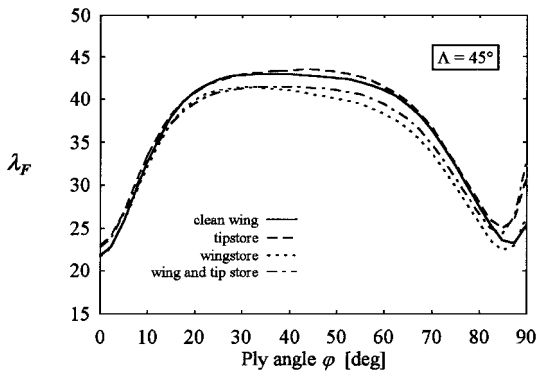

Fig. 11 Effect of ply angle φ on flutter speed parameter $\lambda F = VF/b\omega h$ for a 45-deg swept-back wing (influence of external stores).

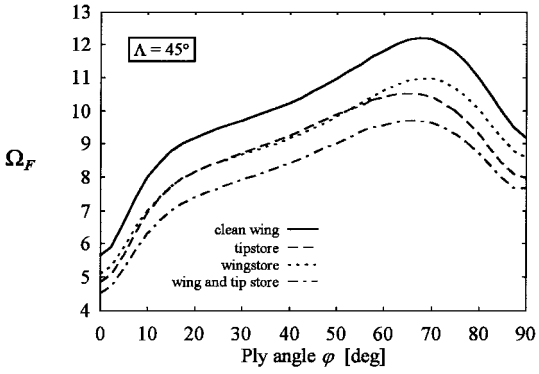

Fig. 12 Effect of ply angle φ on flutter frequency parameter $\Omega F = \omega F/\omega h$ for a 45-deg swept-back wing (influence of external stores).

in this case, mode 2 yields the most critical flutter conditions for all ply-angle orientations.

Conclusions

A well-encompassing structural model of aircraft wings composed of advanced composite anisotropic materials exhibiting transverse shear flexibility and warping inhibition as well as incorporating arbitrarily distributed stores was developed. This model reveals its efficiency in approaching the static and dynamic aeroelasticity of complex wing/store configurations. Results obtained for Goland's[19] and for Goland and Luke's[20] wings via extended Galerkin's method show very good agreement with solutions given by other authors and obtained via completely different approaches to the problem, such as analytical solutions and finite difference or finite element methods. The capability of the model to predict accurately flutter and free vibration behavior of wings carrying external stores is underlined by comparison with theoretical and experimental results for standard unswept metallic wings and composite wings, respectively.

The assumption of a nonshear deformable wing structure ($R = E_1/G_{13} \rightarrow 0$) overestimates divergence and flutter speeds, as well as flutter frequencies. For this reason, to obtain reliable results for static and dynamic aeroelasticity of advanced composite aircraft wings, transverse shear flexibility has to be taken into account. Because wing divergence as a phenomenon is only influenced by wing stiffness parameters, the effect of external stores on the divergence speed has been shown to become immaterial.

The implications of external stores on flutter speed of aeroelastically tailored composite wings can be very complex, depending on the wing/store configuration, because they can be of beneficial or detrimental nature. It has been shown that different store combinations may lead to changes of the critical flutter modes and to discontinuities in the flutter boundary for certain ply angle orientations. In the observed case, increasing the wing sweep from 0 to 45 deg reduces the coupling of the store pitching mode with wing mode 3. As a result, the hump mode causing a discontinuity in the critical flutter speed for the straight wing disappears for the 45-deg

swept-back wing. Therefore, to identify the critical flutter conditions for a composite aircraft wing carrying external stores, it becomes imperative to consider different store configurations already in the preliminary design stages.

Acknowledgment

Frank H. Gern wishes to thank the German Research Society (Deutsche Forschungsgemeinschaft, DFG) for funding his research work under research Grant Ge 923/1-1. This support is highly appreciated.

References

[1]Ruhlin, C. L., Rauch, F. J., Jr., and Waters, C., "Transonic Flutter Study of a Wind-Tunnel Model of a Supercritical Wing with/Without Winglet," AIAA Paper 82-0721, 1982.

[2]Foughner, J. T., and Bensinger, C. T., "F-16 Flutter Model Studies with External Wing Stores," NASA TM 74078, Oct. 1977.

[3]Specialists Meeting on Wing-With-Stores Flutter, CP 162, AGARD, April 1975.

[4]Noll, T. E., Huttsell, L. J., and Cooley, D. E., "Wing/Store Flutter Suppression Investigation," *Journal of Aircraft*, Vol. 18, No. 11, 1981, pp. 969–975.

[5]Försching, H., and Senft, A., "A Parametric Study of the Aeroelastic Stability of a Binary Wing-With-Engine Nacelle Flutter System in Incompressible Flow," *Journal of Flight Sciences and Aerospace Research*, Vol. 16, No. 2, 1994, pp. 77–87.

[6]Weisshaar, T. A., "Aeroelastic Tailoring, Creative Uses of Unusual Materials," AIAA Paper 87-0976, 1987.

[7]Krone, N. J., Jr., "Divergence Elimination with Advanced Composites," AIAA Paper 75-1009, 1975.

[8]Karpouzian, G., and Librescu, L., "Nonclassical Effects on Divergence and Flutter of Anisotropic Swept Aircraft Wings," *AIAA Journal*, Vol. 34, No. 4, 1996, pp. 786–794.

[9]Librescu, L., *Elastostatics and Kinetics of Anisotropic and Heterogeneous Shell-Type Structures*, Noordhoff International, Leyden, The Netherlands, 1975, Chap. 3, pp. 399–456.

[10]Karpouzian, G., and Librescu, L., "Comprehensive Model of Anisotropic Composite Aircraft Wings Suitable for Aeroelastic Analysis," *Journal of Aircraft*, Vol. 31, No. 3, 1994, pp. 703–712.

[11]Gern, F. H., and Librescu, L., "Static and Dynamic Aeroelasticity of Advanced Aircraft Wings Carrying External Stores," *AIAA Journal*, Vol. 36, No. 7, 1998, pp. 1121–1129.

[12]Turner, C. D., "Effect of Store Aerodynamics on Wing/Store Flutter," *Journal of Aircraft*, Vol. 19, No. 7, 1982, pp. 574–579.

[13]Librescu, L., Meirovitch, L., and Song, O., "Refined Structural Modeling for Enhancing Vibrational and Aeroelastic Characteristics of Composite Aircraft Wings," *La Recherche Aérospatiale*, No. 1, 1996, pp. 23–35.

[14]Weisshaar, T. A., "Aeroelastic Tailoring of Forward Swept Composite Wings," *Journal of Aircraft*, Vol. 18, No. 8, 1981, pp. 669–676.

[15]Housner, J. M., and Stein, M., "Flutter Analysis of Swept-Wing Subsonic Aircraft with Parameter Studies of Composite Wings," NASA TN D-7539, Sept. 1974.

[16]Bisplinghoff, R. L., Ashley, H., and Halfman, R. L., *Aeroelasticity*, Addison–Wesley, Reading, MA, 1955, pp. 398, 399, 478.

[17]Runyan, H. L., and Watkins, C. E., "Flutter of a Uniform Wing with an Arbitrarily Placed Mass According to a Differential-Equation Analysis and a Comparison with Experiment," NACA TN 1848, March 1949.

[18]*Manual on Aeroelasticity*, edited by J. W. Jones, Vol. 6, AGARD, 1961, p. 33.

[19]Goland, M., "The Flutter of a Uniform Cantilever Wing," *Journal of Applied Mechanics*, Vol. 12, No. 4, 1945, pp. A-197–A-208.

[20]Goland, M., and Luke, Y. L., "The Flutter of a Uniform Wing with Tip Weights," *Journal of Applied Mechanics*, Vol. 15, No. 1, 1948, pp. 13–20.

[21]Lottati, I., "Aeroelastic Stability Characteristics of a Composite Swept Wing with Tip Weights for an Unrestrained Vehicle," *Journal of Aircraft*, Vol. 24, No. 11, 1987, pp. 793–802.

[22]Lee, I., and Lee, J.-J., "Vibration Analysis of Composite Wing with Tip Mass Using Finite Elements," *Computers and Structures*, Vol. 47, No. 3, 1993, pp. 495–504.